doi:10.1038/nature25159

Strong disk winds traced throughout outbursts in black-hole X-ray binaries

B. E. Tetarenko[1], J.-P. Lasota[2,3], C. O. Heinke[1], G. Dubus[4] & G. R. Sivakoff[1]

Recurring outbursts associated with matter flowing onto compact stellar remnants (such as black holes, neutron stars and white dwarfs) in close binary systems provide a way of constraining the poorly understood accretion process. The light curves of these outbursts are shaped by the efficiency of angular-momentum (and thus mass) transport in the accretion disks, which has traditionally been encoded in a viscosity parameter, α. Numerical simulations[1–3] of the magneto-rotational instability that is believed to be the physical mechanism behind this transport yield values of α of roughly 0.1–0.2, consistent with values determined from observations of accreting white dwarfs[4]. Equivalent viscosity parameters have hitherto not been estimated for disks around neutron stars or black holes. Here we report the results of an analysis of archival X-ray light curves of 21 outbursts in black-hole X-ray binaries. By applying a Bayesian approach to a model of accretion, we determine corresponding values of α of around 0.2–1.0. These high values may be interpreted as an indication either of a very high intrinsic rate of angular-momentum transport in the disk, which could be sustained by the magneto-rotational instability only if a large-scale magnetic field threads the disk[5–7], or that mass is being lost from the disk through substantial outflows, which strongly shape the outburst in the black-hole X-ray binary. The lack of correlation between our estimates of α and the accretion state of the binaries implies that such outflows can remove a substantial fraction of the disk mass in all accretion states and therefore suggests that the outflows correspond to magnetically driven disk winds rather than thermally driven ones, which require specific radiative conditions[8].

The disk-instability model[9–14] was developed to explain outbursts in compact binaries in which a white dwarf accretes from a low-mass companion[15]. A cool (neutral) quiescent disk is built up through steady mass transfer from the companion star, causing the temperature of the disk to increase. At some radius (called the ignition radius), the temperature of the disk will eventually reach the temperature at which hydrogen ionizes. This triggers a thermal–viscous instability within the disk, due to the steep temperature dependence of opacity in this temperature range. As a result, the disk cycles between a hot, ionized, outburst state and a cold, neutral, quiescent state. The growth of the thermal–viscous instability at the ignition radius results in two heating fronts propagating inwards and outwards through the disk. This propagation brings the disk into a hot state, causing rapid in-fall of matter onto the compact object and a bright optical and ultraviolet outburst.

As the disk is depleted over time (because mass falls onto the compact stellar remnant at a higher rate than it is being transferred from the companion star), the temperature and mass-accretion rate in the outer radii will eventually be reduced to the point at which hydrogen can recombine. This triggers the formation and propagation of a cooling front that returns the disk to its quiescent (neutral) state. This predicted behaviour, which is characterized by alternating periods of outbursts and quiescence, matches observations of accreting white dwarfs well. However, changes to the theory are needed for the close binaries known as low-mass X-ray binaries, which contain more compact stellar remnants (such as neutron stars and stellar-mass black holes).

There are 18 confirmed black-hole low-mass X-ray binaries in our Galaxy, identified through bright X-ray outbursts which indicate rapid accretion episodes[16]. These outbursts[16] last considerably longer, and recur much less frequently, than those from many types of accreting white dwarf, owing to heating of the outer disk by X-rays emitted in the inner regions of the accretion flow[17].

X-ray irradiation keeps the accretion disk in its hot (ionized) state over the viscous timescale. This timescale, which is encoded in observed outburst light curves, is related to the efficiency of angular-momentum transport directly and thus provides a means of measuring this efficiency. See Methods and Extended Data Fig. 1 for a detailed discussion of the characteristic three-stage outburst decay profile present in the light curve of a black-hole low-mass X-ray binary.

The magneto-rotational instability is thought to provide the physical mechanism behind angular-momentum (and mass) transport in accretion disks[18]. The effective viscosity in these disks, which is commonly parameterized using the α viscosity prescription[19], encapsulates the efficiency of this transport process. Physically, the viscosity parameter α sets the viscous time of the accretion flow through the disk and thus, according to the disk-instability model, is encoded within the decay profile of the light curve of an outburst. A disk with higher viscosity (higher α) in outburst will accrete mass more quickly, resulting in shorter decay times and shorter outburst durations[20].

The α viscosity has been inferred only in (non-irradiated) disks around accreting white dwarfs, by comparing the outburst timescales from observed light curves to synthetic model light curves created by numerical disk codes for different α inputs[4]. Values of α have not previously been measured in irradiated accretion disks, such as those around stellar-mass black holes in low-mass X-ray binaries. The assertion[21] that $\alpha \approx 0.2$–0.4 in such systems was deduced from calculations[20] of "detailed models of complete light curves", not from detailed comparison of models with observations. Note that we learned of a recent study[22] of the black-hole low-mass X-ray binary 4U 1543–475 after acceptance of this manuscript.

Accordingly, we have built a Bayesian approach that characterizes the angular-momentum (and mass) transport that occurs in disks in low-mass X-ray binary systems. The α viscosity parameter in a hot, outbursting disk ($\alpha_{\rm h}$) sets the timescale on which matter moves through the hot (ionized) portion of the disk and thus controls the duration of the first stage of the decay profile observed in an X-ray light curve (see Methods for details). This (viscous) timescale varies depending on the mass of the compact object and the size of the accretion disk, with the size of the disk itself governed by the ratio of component masses in the system and the orbital period of the binary. To reconcile the multi-level, interconnected relationships that exist between these parameters that define the properties of the accretion flow, we use Bayesian

[1]Department of Physics, University of Alberta, CCIS 4-181, Edmonton, Alberta T6G 2E1, Canada. [2]Institut d'Astrophysique de Paris, CNRS et Sorbonne Universités, UPMC Paris 06, UMR 7095, 98bis Boulevard Arago, 75014 Paris, France. [3]Nicolaus Copernicus Astronomical Centre, Polish Academy of Sciences, ulica Bartycka 18, 00-716 Warsaw, Poland. [4]Université Grenoble Alpes, CNRS, Institut de Planétologie et d'Astrophysique de Grenoble (IPAG), F-38000 Grenoble, France.

© 2018 Macmillan Publishers Limited, part of Springer Nature. All rights reserved.

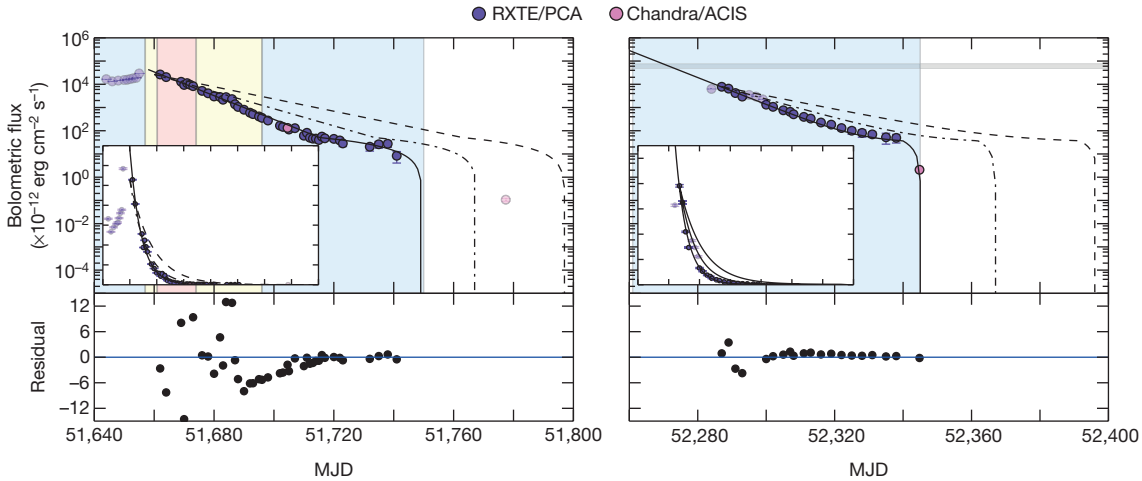

Figure 1 | Example light curves of outbursts in low-mass X-ray binaries. The figure displays the observed bolometric X-ray light curves for the 2000 (left) and 2001–2002 (right) outbursts of the low-mass X-ray binary XTE J1550−564, which harbours a black hole with a mass of 10.4 ± 2.3 solar masses ($M_{\odot}$)[16]. In this source, which has undergone multiple outbursts in the past two decades, we measure an extremely high value of the viscosity parameter α. Shading in the background indicates the accretion state of the source during the outbursts: blue, hard; yellow, intermediate; red, soft. Although XTE J1550−564 transitions from the soft to hard accretion state during the decay of the 2000 outburst, the light curve shows no signature of that transition. Disk outflows have been observed only in the soft and intermediate states, or at high flux levels (greater than 10% Eddington)[27], above the grey bar (left) in the hard state. Coloured circles represent data from different X-ray instruments: the Proportional Counter Array aboard the Rossi X-ray Timing Explorer (RXTE/PCA), or the Advanced CCD Imaging Spectrometer aboard the Chandra X-ray Observatory (Chandra/ACIS). Translucent data indicate the rise of the outburst, which was not included in the fits. Error bars show the statistical uncertainties of the instruments. The insets show the outbursts on a linear scale. The best-fitting analytical model (solid black line) and residuals (lower panel) are displayed in both panels. We measure $\alpha_h = 0.96 \pm 0.15$ and $\alpha_h = 0.99^{+0.15}_{-0.14}$ from the light curves of the 2000 and 2001–2002 outbursts, respectively. We over-plot the resulting decay profiles corresponding to $\alpha_h = 0.7$ (dot-dashed line) and $\alpha_h = 0.5$ (dashed line), demonstrating the way in which the shape of the light curve changes with different values of α. MJD, modified Julian date.

hierarchical modelling (see Methods of details). This technique allows us to derive: (i) the timescales associated with individual stages of the decay of the outburst, and (ii) the rate of mass accretion through the disk during, and the time of occurrence of, the transitions between the individual decay stages. Ultimately, the Bayesian technique allows us to take into account effectively our prior knowledge of the orbital parameters that define a low-mass X-ray binary system (black-hole mass, companion mass and orbital period) and thus to sample α_h directly from its observed X-ray light curve.

We analysed a representative sample of X-ray light curves of 21 individual outbursts of 12 black-hole low-mass X-ray binary systems from the WATCHDOG project[16] (Extended Data Table 1). In Fig. 1 we show examples of the analytical irradiated-disk-instability model fitted to observed data. In this figure, we overlay predicted decay profiles that illustrate the way in which varying α_h changes the predicted light-curve decay profile. For these 21 outbursts, we derive $0.19 < \alpha_h < 0.99$ (see Fig. 2 and Extended Data Table 2). These results represent a derivation of α in accretion disks of low-mass X-ray binaries from a fit to the observed light curves of outbursts in such systems.

There are two possible explanations for the high values of α that we measure. The first is that we really are measuring the intrinsic value of α for these disks. The only way to reproduce such high intrinsic values of α in accretion-disk simulations is for a net magnetic field to thread the disk, with concurrent mass outflows strongly shaping the outburst as a whole. Simulations of angular-momentum transport driven by the magneto-rotational instability, carried out in vertically stratified boxes that represent a local patch of the disk (shearing box), typically yield $\alpha \approx 0.02$ without a net magnetic flux[23,24]. Convection enhances transport to yield $\alpha \approx 0.2$ in the conditions appropriate to accreting white dwarfs[1–3]. This value is consistent with those deduced from observations of outbursts in the non-irradiated disks around these objects[4], but is insufficient to explain the higher values of $\alpha \gtrsim 0.2$ that we measure from outbursts in black holes. However, when the shearing box is threaded by a net magnetic flux, simulations show that α scales as $\beta^{-1/2}$ (where β is the ratio of the thermal pressure

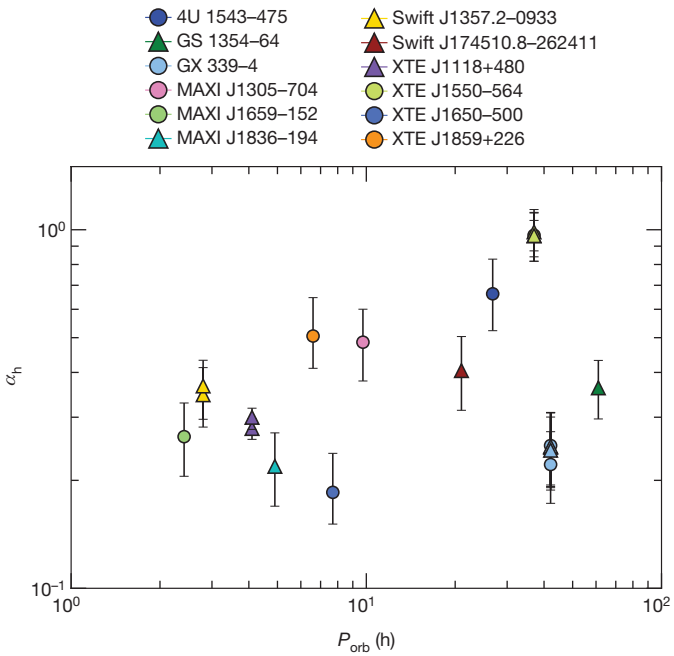

Figure 2 | Characterization of the mass-transport process in accretion disks. The α viscosity parameter in the hot, ionized zone of the disk (α_h), which encompasses the efficiency of angular-momentum (and mass) transport in accretion disks, as derived using our Bayesian methodology, is plotted against the orbital period (P_{orb}) of the binary system, for the 21 individual outbursts that occurred in our sample of 12 Galactic black-hole low-mass X-ray binaries with measured orbital periods. The different colours represent individual sources. Error bars represent the 68% confidence interval. The values of α_h are derived both for outbursts during which the source cycles through all accretion states (hard, intermediate and soft; circles) and for those during which the source remains in the hard accretion state (triangles).

© 2018 Macmillan Publishers Limited, part of Springer Nature. All rights reserved.

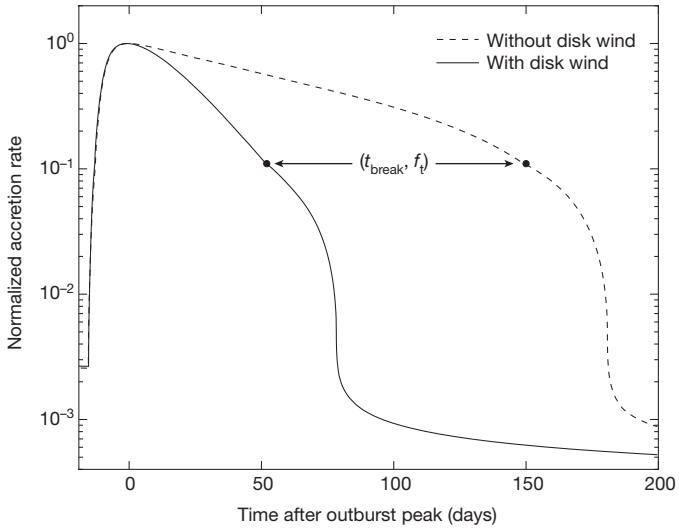

Figure 3 | Toy model of a disk 'wind'. Two model light curves for an irradiated disk with $\alpha_h = 0.2$ around a $6M_\odot$ black hole are shown: dashed line, assuming no mass loss; solid line, including a term to account for mass loss during the outburst. The latter is computed assuming mass loss is proportional to the central mass-accretion rate onto the black hole ($\dot{M}_w = \varepsilon_w \dot{M}_c$) during the decay (meant to be representative of a disk-wind-type outflow). Although the shape of the profile remains the same, the effective timescale τ_e is reduced to $(1-\varepsilon_w)\tau_e$. Thus, as the fraction of mass lost increases, τ_e decreases, mimicking the effect an arbitrary large value of α has on the light-curve profile (that is, high α corresponds to fast decay). A measurement of $\alpha = 1$ would correspond to a disk with $\alpha = 0.2$ and $\varepsilon_w = 0.8$ in the toy model, indicative of a substantial outflow. Note that, although this model assumes that the local outflow rate is related to the local accretion rate in the disk, this need not be the case. Further, this simplifying assumption, used purely to solve for the light curve numerically, limits what we can say about how much mass is lost in the outflow. This model requires $\dot{M}_w/\dot{M}_c < 1$, but it is certainly possible that the outflow rate is larger than the central mass-accretion rate onto the black hole ($\dot{M}_w/\dot{M}_c > 1$). The transition (which occurs at a flux f_t and time t_{break}) between the viscous and irradiation-controlled stages of the decay in each light-curve is indicated by a black filled circle.

to the imposed magnetic pressure), reaching values as high as $\alpha \approx 1$ when β is roughly 1–10^3, with $\beta = 1$ the lower limit for the magneto-rotational instability to operate in a thin disk[5–7]. Hence, strong intrinsic angular-momentum transport indicates the presence of a large-scale field in the accretion disk, origin and evolution of which have yet to be determined in black-hole transients. Moreover, simulations that reproduce high intrinsic α also display strong outflows, which actually do not remove much angular momentum; thus, angular-momentum transport is still primarily driven by the magneto-rotational instability.

The second possibility is that the intrinsic values of α for accretion disks of black-hole low-mass X-ray binaries are smaller than we measure (for example, comparable to 0.2) and that unspecified strong mass outflows are shaping the overall light-curve profiles that we observed. Figure 3 illustrates how including a term to account for mass (and angular-momentum) loss within the irradiated-disk-instability model results in a model that mimics the effect that high α has on the light-curve decay profile.

In both cases, substantial outflows appear to have a key role in regulating the disk-accretion process. Strong mass outflows have been observed in outbursting low-mass X-ray binaries in the soft or intermediate accretion states, or at high flux levels (greater than 10% Eddington) in the hard accretion state[25–27], in the form of accretion-disk winds. These outflows have been attributed to thermal winds driven by X-ray irradiation or to magnetic winds driven by centrifugal acceleration along magnetic field lines anchored in the disk[8,28]. It has recently been shown that thermally driven winds (such as Compton-heated winds[26]) can be produced only in the soft accretion state, because the ionization state of the wind becomes unstable in the hard accretion state (see, for example, refs 29, 30). The absence of a correlation between the values of α and the X-ray flux or accretion state in our outburst sample suggests that the outflow mechanism is generic, and favours magnetically driven over thermally driven outflows.

Online Content Methods, along with any additional Extended Data display items and Source Data, are available in the online version of the paper; references unique to these sections appear only in the online paper.

Received 7 September; accepted 17 November 2017.
Published online 22 January 2018.

1. Hirose, S., Blaes, O., Krolik, J., Coleman, M. & Sano, T. Convection causes enhanced magnetic turbulence in accretion disks in outburst. *Astrophys. J.* **787,** 1 (2014).
2. Coleman, M., Kotko, I., Blaes, O., Lasota, J.-P. & Hirose, S. Dwarf nova outbursts with magnetorotational turbulence. *Mon. Not. R. Astron. Soc.* **462,** 3710–3726 (2016).
3. Scepi, N., Lesur, G., Dubus, G. & Flock, M. Impact of convection and resistivity on angular momentum transport in dwarf novae. *Astron. Astrophys.* https://doi.org/10.1051/0004-6361/201731900 (2017).
4. Kotko, I. & Lasota, J.-P. The viscosity parameter and the properties of accretion disc outbursts in close binaries. *Astron. Astrophys.* **545,** A115 (2012).
5. Lesur, G., Ferreira, J. & Ogilvie, G. I. The magnetorotational instability as a jet launching mechanism. *Astron. Astrophys.* **550,** A61 (2013).
6. Bai, X.-N. & Stone, J. Local study of accretion disks with a strong vertical magnetic field: magnetorotational instability and disk outflow. *Astrophys. J.* **767,** 30–48 (2013).
7. Salvesen, G., Simon, J. B., Armitage, P. J. & Begelman, M. C. Accretion disc dynamo activity in local simulations spanning weak-to-strong net vertical magnetic flux regimes. *Mon. Not. R. Astron. Soc.* **457,** 857–874 (2016).
8. Higginbottom, N. & Proga, D. Coronae and winds from irradiated disks in x-ray binaries. *Astrophys. J.* **807,** 107–116 (2015).
9. Osaki, Y. An accretion model for the outbursts of U Geminorum stars. *Publ. Astron. Soc. Jpn* **26,** 429–436 (1974).
10. Meyer, F. & Meyer-Hofmeister, E. On the elusive cause of cataclysmic variable outbursts. *Astron. Astrophys.* **104,** 10–12 (1981).
11. Smak, J. Accretion in cataclysmic binaries. IV. Accretion disks in dwarf novae. *Acta Astron.* **34,** 161–189 (1984).
12. Faulkner, J., Lin, D. N. C. & Papaloizou, J. On the evolution of accretion disc flow in cataclysmic variables – I. The prospect of a limit cycle in dwarf nova systems. *Mon. Not. R. Astron. Soc.* **205,** 359–375 (1983).
13. Huang, M. & Wheeler, J. Thermal instability accretion disk model for the X-ray transient A0620−00. *Astrophys. J.* **343,** 229–240 (1989).
14. Cannizzo, J. K. *Accretion Disks in Compact Stellar Systems* (World Scientific, 1993).
15. Warner, B. *Cataclysmic Variable Stars* Ch. 3, 126–215 (Cambridge Univ. Press, 1995).
16. Tetarenko, B., Sivakoff, G., Heinke, C. & Gladstone, J. C. Watchdog: a comprehensive all-sky database of galactic black hole x-ray binaries. *Astrophys. J. Suppl. Ser.* **222,** 15 (2016).
17. van Paradijs, J. On the accretion instability in soft x-ray transients. *Astrophys. J.* **464,** L139–L141 (1996).
18. Balbus, S. & Hawley, J. Instability, turbulence, and enhanced transport in accretion disks. *Rev. Mod. Phys.* **70,** 1–53 (1998).
19. Shakura, N. I. & Sunyaev, R. A. Black holes in binary systems. Observational appearance. *Astron. Astrophys.* **24,** 337–355 (1973).
20. Dubus, G., Hameury, J.-M. & Lasota, J.-P. The disc instability model for x-ray transients: evidence for truncation and irradiation. *Astron. Astrophys.* **373,** 251–271 (2001).
21. King, A. R., Pringle, J. E. & Livio, M. Accretion disc viscosity: how big is alpha? *Mon. Not. R. Astron. Soc.* **376,** 1740–1746 (2007).
22. Lipunova, G. V. & Malanchev, K. L. Determination of the turbulent parameter in accretion discs: effects of self-irradiation in 4U 1543−47 during the 2002 outburst. *Mon. Not. R. Astron. Soc.* **468,** 4735–4747 (2017).
23. Davis, S. W., Stone, J. M. & Pessah, M. E. Sustained magnetorotational turbulence in local simulations of stratified disks with zero net magnetic flux. *Astrophys. J.* **713,** 52–65 (2010).
24. Simon, J. B., Beckwith, K. & Armitage, P. J. Emergent mesoscale phenomena in magnetized accretion disc turbulence. *Mon. Not. R. Astron. Soc.* **422,** 2685–2700 (2012).
25. Miller, J. M. *et al.* Simultaneous Chandra and RXTE spectroscopy of the microquasar H1743−322: clues to disk wind and jet formation from a variable ionized outflow. *Astrophys. J.* **646,** 394–406 (2006).
26. Ponti, G. *et al.* Ubiquitous equatorial accretion disc winds in black hole soft states. *Mon. Not. R. Astron. Soc.* **422,** L11–L15 (2012).
27. Neilsen, J. The case for massive, evolving winds in black hole x-ray binaries. *Adv. Space Res.* **52,** 732–739 (2013).
28. Ohsuga, K. & Mineshige, S. Global structure of three distinct accretion flows and outflows around black holes from two-dimensional radiation-magnetohydrodynamic simulations. *Astrophys. J.* **736,** 2 (2011).

© 2018 Macmillan Publishers Limited, part of Springer Nature. All rights reserved.

29. Chakravorty, S., Lee, J. C. & Neilsen, J. The effects of thermodynamic stability on wind properties in different low-mass black hole binary states. *Mon. Not. R. Astron. Soc.* **436,** 560–569 (2013).
30. Bianchi, S., Ponti, G., Muñoz-Darias, T. & Petrucci, P.-O. Photoionization instability of the Fe K absorbing plasma in the neutron star transient AX J1745.6−2901. *Mon. Not. R. Astron. Soc.* **472,** 2454–2461 (2017).

Acknowledgements B.E.T. thanks participants of the 'disks17: Confronting MHD Theories of Accretion Disks with Observations' programme, held at the Kavli Institute for Theoretical Physics (KITP), for their feedback and comments on this project, especially A. Veledina for advice regarding the analysis of the X-ray light curves and P. Charles for comments on the manuscript. B.E.T., G.R.S. and C.O.H. acknowledge support by NSERC Discovery Grants, and C.O.H. by a Discovery Accelerator Supplement. This research was supported in part by the National Science Foundation under grant number NSF PHY-1125915, via support for KITP. J.-P.L. acknowledges support by the Polish National Science Centre OPUS grant 2015/19/B/ST9/01099. J.-P.L. and G.D. also acknowledge support from the French Space Agency CNES. This research has made use of data, software, and/or web tools obtained from the High Energy Astrophysics Science Archive Research Center (HEASARC), a service of the Astrophysics Science Division at NASA/GSFC and of the Smithsonian Astrophysical Observatory's High Energy Astrophysics Division, data supplied by the UK Swift Science Data Centre at the University of Leicester, and data provided by RIKEN, JAXA and the MAXI team. This work has also made extensive use of NASA's Astrophysics Data System (ADS).

Author Contributions B.E.T. performed the analysis of the X-ray data, wrote the Markov chain Monte Carlo light-curve-fitting algorithm and performed the light-curve fitting, built the Bayesian hierarchical methodology and wrote the paper. J.-P.L. helped to formulate the analytical version of the irradiated-disk-instability model that was fitted to the X-ray light curves, contributed to the interpretation of the data and assisted in writing the discussion in the paper. C.O.H. assisted in the analysis of the X-ray data and the light-curve-fitting process, and contributed to the interpretation of the data. G.D. contributed to the interpretation of the data and assisted in writing the discussion in the paper. G.R.S. assisted in writing the paper and contributed to the interpretation of the data.

Author Information Reprints and permissions information is available at www.nature.com/reprints. The authors declare no competing financial interests. Readers are welcome to comment on the online version of the paper. Publisher's note: Springer Nature remains neutral with regard to jurisdictional claims in published maps and institutional affiliations. Correspondence and requests for materials should be addressed to B.E.T. (btetaren@ualberta.ca).

Reviewer Information *Nature* thanks D. Proga and the other anonymous reviewer(s) for their contribution to the peer review of this work.

© 2018 Macmillan Publishers Limited, part of Springer Nature. All rights reserved.

METHODS

Archival X-ray data collection and reduction. We have collected all outburst data available since 1996, for each of the 12 systems in our source sample, from (i) the Proportional Counter Array (PCA) aboard the Rossi X-ray Timing Explorer (RXTE), (ii) the X-ray Telescope (XRT) aboard the Swift Observatory, (iii) the Gas-Slit Camera (GSC) aboard the Monitor of All-sky Image (MAXI) Telescope, (iv) the Advanced CCD Imaging Spectrometer (ACIS-S) and High Resolution Camera (HRC-S) aboard the Chandra X-ray Observatory, and (v) the European Photon Imaging Camera (EPIC) aboard XMM-Newton.

All X-ray light-curve data from RXTE/PCA was collected from the WATCHDOG project[16]. These authors compiled all available good pointed PCA observations (no scans or slews) from the HEASARC archive, for 77 black-hole X-ray binary sources in the Galaxy, over the entire 16-year RXTE mission. For each individual source in our sample, we use scripts from the WATCHDOG project, including the *rex* script within the Heasoft Software Package (http://heasarc.nasa.gov/lheasoft/), to reduce and extract (mission-long) daily time-binned, background-subtracted light curves in the 2–10-keV band from the PCA Std2 data available on that source in the WATCHDOG database. We also compiled all available MAXI/GSC data using the WATCHDOG project's online light-curve tool (http://astro.physics.ualberta.ca/WATCHDOG). This tool compiles all of the publicly available data from the MAXI archive (http://maxi.riken.jp/top/) in three standard bands (2–4 keV, 4–10 keV, 10–20 keV) and runs it through the WATCHDOG processing pipeline[16]. Using this tool, we extracted (mission-long) daily time-binned, background-subtracted light curves in the 2–10-keV band for each individual source (where available).

In addition, we use the Swift/XRT online product builder[31,32] (http://www.swift.ac.uk/user_objects/index.php) to compile (mission-long) daily time-binned, background-subtracted light curves in the 2–10-keV band, using all available windowed-timing- and photon-counting-mode XRT pointed observations. Last, we collected all available Chandra/ACIS-S, Chandra/HRC-S and XMM-Newton/EPIC pointed observations from the literature for individual outbursts (where available). We then convert individual instrument count rates to fluxes in the 2–10-keV band using PIMMS v4.8c (http://cxc.harvard.edu/toolkit/pimms.jsp) and the spectral information available in the literature.

Conversion from count rate to bolometric flux. We use crabs as a baseline unit of flux to calculate approximate count-rate equivalences in the 2–10-keV-band data from RXTE/PCA, Swift/XRT and MAXI/GSC. Integration of the now-accepted, 'canonical', simple power-law spectrum of the Crab Nebula[33] over the 2–10-keV band gives us a straightforward method for converting between count rate and flux in this band. Assuming that a source spectrum is Crab-like in nature results in uncertainty in the computed source flux. However, given that it has been found that assuming a Crab-like spectral shape in narrow X-ray energy bands (such as the 2–10-keV band we make use of here) produces no more than a 20% (and typically less than 10%) error in the source flux for a flat power law versus a blackbody[16], this approach is justified.

To convert flux in the 2–10-keV band to bolometric flux, we use the following bolometric corrections (BCs), estimated for each individual accretion state[34] that occurs during outbursts of black-hole low-mass X-ray binaries: hard state, BC = 5; soft and intermediate states, BC = 1.25. By combining the bolometric corrections discussed above with the daily accretion-state information for each outburst, obtained from the WATCHDOG project's[16] online Accretion-State-By-Day tool (http://astro.physics.ualberta.ca/WATCHDOG), we are able to compute daily time-binned bolometric light curves.

Markov chain Monte Carlo (MCMC) fitting algorithm. We use a Bayesian approach to estimate the five parameters that describe the shape of an observed light-curve decay profile: (i) the exponential (viscous) decay timescale (τ_e), (ii) the linear (irradiation-controlled) decay timescale (τ_l), (iii) the X-ray flux of the system at the transition between exponential and linear decay stages (f_t), (iv) the time after the outburst peak when the transition between exponential and linear decay stages occurs (t_{break}), and (v) the X-ray flux limit of the exponential decay stage (f_2); see Extended Data Fig. 1. Using the *emcee* python package[35], an implementation of the Affine Invariant MCMC Ensemble Sampler[36], we apply a MCMC algorithm to fit the exponential (viscous) and linear (irradiation-controlled) stages of each decay simultaneously (as described in the main text and Extended Data Fig. 1), where applicable.

Before fitting occurs, secondary maxima and other rebrightening events[20,37,38] that contaminate the decays are removed by hand. These data are not included in the fits; analysis of these rebrightening events will be presented in a later paper. The removal of these rebrightening events has no effect on the determination of α from the X-ray light curves. The remaining data are then fitted in logarithmic (bolometric) flux space with our five-parameter analytical model (see below for details).

The *emcee* python package runs a modified version of the Metropolis–Hastings algorithm, in which an ensemble of 'walkers' move simultaneously through and explore the parameter space. To fit each light curve, we use 50 walkers—10 times the dimension of model. For *emcee* to run optimally, we first set the initial positions of our ensemble of walkers appropriately in parameter space. To do so, we use *pyHarmonySearch*[39], an implementation of the harmony search global optimization algorithm, to perform an initial survey of our parameter space. *pyHarmonySearch* acts essentially as a less-time-consuming version of a brute-force grid-search method, allowing us to place our ensemble of walkers in a tight ball around the best guess that it finds. This best guess provides a starting point for the MCMC algorithm.

Prior distributions for each of the five parameters are also set from the results of *pyHarmonySearch*. In the case of a well-sampled light curve (near-continuous daily data throughout the outburst), a Gaussian prior for each parameter with a mean set by the results of *pyHarmonySearch* is used. In the case in which only scattered data are available on only a portion of the full decay, wide flat priors (based on expectations from other outbursts of the same source, or outbursts from sources with similar orbital periods) are used for each parameter.

After initialization, we begin running the MCMC algorithm on each light curve with a 500-step burn-in phase. Here the ensemble of walkers are evolved over a series of steps to ensure that the initial configuration that we have set enables the walkers to explore the parameter space sufficiently. At the end of the burn-in phase, if the initial configuration is appropriate for the problem, the walkers will have ended up in a high-probability region, a place in parameter space in which the states of the Markov chain are more representative of the distribution being sampled. After this phase, the MCMC algorithm is restarted, with the walkers starting at the final position they acquired during the burn-in phase, and run until convergence. The number of steps required for convergence depends on the amount of data available and the complexity of the decay profile of the outburst.

After likelihood maximization is performed, the MCMC algorithm outputs the converged solution in the form of posterior distributions of each parameter. We take the best-fit result (the best-fit value along with the upper and lower limits on this value) as the median and 1σ (68%) confidence interval of each posterior distribution, respectively.

The analytical outburst decay model. Extended Data Fig. 1 shows the predicted characteristic three-stage decay profile shape present in the light curve of a black-hole low-mass X-ray binary[20,37,40].

In the first stage (viscous decay), X-ray irradiation keeps the whole disk in a hot (ionized) state, preventing the formation of a cooling front. As more mass is accreted onto the black hole than is transferred from the companion at this time, the disk is drained by viscous accretion of matter only, resulting in an exponential-shaped decay profile on the viscous timescale. Eventually, as the mass in the disk and the mass transfer rate decrease, the dimming X-ray irradiation can no longer keep the outer regions of the disk in the hot (ionized) state and a cooling front forms, behind which the cold matter slows its inward flow drastically. At this point, the system enters the second stage (irradiation-controlled decay), during which the propagation of the cooling front is controlled by the decay of the irradiating X-ray flux. The hot (ionized) portion of the disk continues to flow and accrete, but gradually shrinks in size, causing a linear-shaped decay profile. Eventually, the mass accretion rate onto the black hole becomes small enough that X-ray irradiation no longer has a role. In this third and final stage (thermal decay), the cooling front propagates inward freely on a thermal–viscous timescale, resulting in a steeper linear decay in the light curve down to the quiescent accretion level.

The analytical model that we use to describe the outburst decay profiles in the light curves of black-hole low-mass X-ray binaries, predicted by the (irradiated) disk-instability model, is rooted in the 'classic' King and Ritter formalism[37]. This formalism combines knowledge of the peak X-ray flux and of the outer radius of the irradiated disk to predict the shape that the decay of an X-ray light curve of a transient low-mass X-ray binary system would follow.

The temperature of most of the accretion disk in transient low-mass X-ray binaries during outburst is dominated by X-ray heating from the inner accretion region. The X-ray light curve will show an exponential decline if irradiation by the central X-ray source is able to ionize the entire disk, keeping it in the hot (ionized) state and preventing the formation of the cooling front[41]. The X-ray light curve will show a linear decline if irradiation by the central X-ray source is able to keep only a portion of the entire disk in the hot (ionized) state. In this case, the central X-ray flux will no longer be able to keep the outer regions of the disk above the hydrogen ionization temperature (around 10^4 K) and a cooling front will appear and propagate down the disk. Because the cooling front cannot move inward on a viscous timescale (the farthest it can move inward is set by the radius at which $T = 10^4$ K), a linear-shaped decline is observed in the light curve.

© 2018 Macmillan Publishers Limited, part of Springer Nature. All rights reserved.

By assuming, as do many studies of X-ray irradiated disks in close binary systems, an isothermal disk model (that is, the disk is assumed to be vertically isothermal because it is irradiated, with the central mid-plane temperature equal to the effective temperature set by the X-ray irradiation flux at the disk surface[42]), the critical X-ray luminosity for a disk radius R_{11} (in units of 10^{11} cm) has been derived[37] to be $L_{\rm crit,BH} = 1.7 \times 10^{37}\ R_{11}^2$ erg s^{-1}, above which the light curve should display an exponential decay shape and below which the light curve should display a linear decay shape. In this formalism, a well-sampled light curve (in both time and amplitude) should show a combination of exponential- and linear-shaped stages in the decay profile. The exponential decay is replaced with a linear decay when the X-ray flux has decreased sufficiently, resulting in a distinct brink (such as a break in slope) in the light-curve shape. By deriving analytical expressions for the shape that light-curve decays of transient low-mass X-ray binaries systems take, the timescales of the exponential and linear stages of a decay, the peak mass-accretion rate (and in-turn X-ray luminosity for a given accretion efficiency) and the time at which the exponential decay is replaced by the linear decay have been predicted[37].

This approach has since been validated by smooth-particle-hydrodynamics accretion simulations[43] and applied to observations of various classes of X-ray binaries[44–49] with varied success. However, although the King and Ritter formalism has, coincidentally, been found to agree relatively well with observations, it oversimplifies the physics of the X-ray-irradiated disks to which it is applied[41]. Therefore, we instead use a modified version of the King and Ritter formalism.

In this modified version we (i) include the effects of continuing mass transfer from the donor star[47,48], and (ii) use a disk structure[20,40] in which X-ray irradiation that affects the disks of black-hole low-mass X-ray binaries is modelled using a general irradiation law:

$$T_{\rm irr}^4 = \frac{C_{\rm irr} L_{\rm X}}{4\pi\sigma R^2}$$

Here, the irradiation parameter $C_{\rm irr}$ is defined as the fraction of the central X-ray luminosity ($L_{\rm X} = \eta c^2 \dot{M}_{\rm c}$ for accretion efficiency η) that heats up the disk. Because $C_{\rm irr}$ contains information about the illumination and disk geometry, and the temperature profile of the X-ray irradiation, it effectively parameterizes our ignorance of how these disks are actually irradiated. Physically, $C_{\rm irr}$ controls the timescale of the linear decay stage (and the overall outburst duration) and when the transition between decay stages occur, and sets a limit on the amount of mass that can be accreted during the outburst. Stronger irradiation (larger $C_{\rm irr}$) increases the duration of the outburst and thus the relative amount of matter able to be accreted during an outburst. Consequently, if more matter is accreted during outburst, the subsequent time in quiescence will lengthen because the disk will require more time to build up again.

Following the procedure outlined in previous work[47,48], but instead using the general irradiation law defined above, yields the following analytical form for the flux of a black-hole low-mass X-ray binary as a function of time during the exponential (viscous) and linear (irradiation-controlled) stages of the decay:

$$f_{\rm X} = \begin{cases} (f_{\rm t} - f_2)\exp\left(-\dfrac{t - t_{\rm break}}{\tau_{\rm e}}\right) + f_2 \\ f_{\rm t}\left(1 - \dfrac{t - t_{\rm break}}{\tau_{\rm l}}\right) \end{cases}$$

Here $\tau_{\rm e}$ and $\tau_{\rm l}$ are defined as the viscous (exponential) decay timescale in the hot (ionized) zone of the disk and the linear decay timescale, respectively; $f_2 = \eta c^2(-\dot{M}_2)/(4\pi d^2)$ is the flux limit of the exponential decay, which depends on the mass-transfer rate from the companion $-\dot{M}_2$ and the distance to the source d; $t_{\rm break}$ is defined as the time when the temperature of the outer edge of the disk is just sufficient to remain in a hot (ionized) state; and $f_{\rm t}$ is the corresponding X-ray flux of the system at time $t_{\rm break}$. We perform fits in flux, as opposed to luminosity, space to avoid the correlated errors (due to an uncertain distance) that would arise if we were to fit the latter; the uncertain distance (and other parameters) are incorporated below.

By fitting this model to our sample of observed X-ray light curves we can derive the viscous decay timescales in black-hole low-mass X-ray binaries to range between roughly 50 and 190 days, consistent with previous conclusions[50]; see Extended Data Table 2 for fit results.

The Bayesian hierarchical methodology. We quantify the angular-momentum (and mass) transport that occurs in the irradiated accretion disks in low-mass X-ray binary systems using the α viscosity parameter. In the current form of the disk-instability model, the use of this simple parameter results from the inability of current numerical simulations to follow *ab initio* turbulent transport driven by the magneto-rotational instability on viscous timescales in a global model of the accretion disk.

This parameter is encoded within the viscous (exponential) stage of the light-curve decay profile. During this first stage of the decay, irradiation of the disk traps it in a hot (ionized) state that allows a decay of the central mass-accretion rate only on a viscous timescale: $\tau_{\rm e} = R_{\rm h,disc}^2/(3\nu_{\rm KR})$, where $\nu_{\rm KR}$ is the Shakura–Sunyaev viscosity[19], the average value of the kinematic viscosity coefficient near the outer edge of the disk[37], and $R_{\rm h,disk}$ is the radius of the hot (ionized) zone of the disk. For Keplerian disks, the Shakura–Sunyaev viscosity is related to the dimensionless viscosity parameter in the hot disk $\alpha_{\rm h}$ by $\nu_{\rm KR} = \alpha_{\rm h} c_{\rm s}^2/\Omega_{\rm k}$, where $\Omega_{\rm k}$ is the Keplarian angular velocity and $c_{\rm s}$ is the sound speed in a disk (proportional to $T_{\rm c}^{0.5}$, where $T_{\rm c}$ is the central mid-plane temperature of the disk). Therefore, using $\Omega_{\rm k} = (GM_1/R^3)^{1/2}$, the viscous timescale in the disk can be written as a function of $\alpha_{\rm h}$, the mass of the compact object M_1 and the radius of the accretion disk $R_{\rm h,disk}$:

$$\left(\frac{\tau_{\rm e}}{\rm s}\right) = \left(\frac{G^{0.5} m_{\rm H} M_\odot^{0.5}(10^6)}{3\gamma k_{\rm B} T_{\rm c}}\right)\left(\frac{\alpha_{\rm h}}{0.1}\right)^{-1}\left(\frac{M_1}{M_\odot}\right)^{0.5}\left(\frac{R_{\rm h,disk}}{10^{10}\ {\rm cm}}\right)^{0.5}$$

where G is the gravitational constant, $m_{\rm h}$ is the mass of a hydrogen atom, γ is the adiabatic index (the ratio of the specific heats of a gas at a constant pressure and a gas at a constant volume) and $k_{\rm B}$ is the Boltzmann constant. Because $T_{\rm c}$ is only weakly dependent on viscosity and X-ray irradiation in irradiated disks, we can approximate its value as a constant, 16,300 K (ref. 51).

Solving for $\alpha_{\rm h}$ yields

$$\left(\frac{\alpha_{\rm h}}{0.1}\right) = \left(\frac{G^{0.5} m_{\rm H} M_\odot^{0.5}(10^6)}{3\gamma k_{\rm b} T_{\rm c}}\right)\left(\frac{\tau_{\rm e}}{\rm s}\right)^{-1}\left(\frac{M_1}{M_\odot}\right)^{0.5}\left(\frac{R_{\rm h,disk}}{10^{10}\ {\rm cm}}\right)^{0.5}$$

Because $\alpha_{\rm h}$ depends on parameters that characterize the outburst decay profile of a low-mass X-ray binary (that is, observed data) as well as on the orbital parameters that define the binary system (that is, parameters that we have prior knowledge of, namely, M_1 and $R_{\rm h,disk}$, which is itself dependent on M_1, the mass of the companion star in the system and the orbital period $P_{\rm orb}$), we require a multi-level Bayesian statistical sampling technique to effectively sample $\alpha_{\rm h}$.

We therefore built a Bayesian hierarchical model. A Bayesian hierarchical model is a multi-level statistical model that enables the posterior distribution of some quantity to be estimated by integrating a combination of known prior distributions with observed data. In our case, the established orbital parameters of the binary (M_1, binary mass ratio q, $P_{\rm orb}$) for a system act as the known priors, and the quantitative outburst decay properties derived from fitting the light curves of a low-mass X-ray binary system with the analytical version of the irradiated disk-instability model that we developed ($\tau_{\rm e}$) act as the observed data.

Using *emcee*[35] (see above for details), our hierarchical model samples $\alpha_{\rm h}$ simultaneously for all outbursts of each of the 12 sources in our sample using 240 walkers, 10 times the dimension of our model: 12 of these dimensions correspond to 6 established measurements of black-hole mass, 4 known binary mass ratios and 2 observationally based Galactic statistical population distributions (the Özel black-hole mass distribution[52] and the distribution of binary mass ratios for the dynamically confirmed stellar-mass black holes in the Galaxy[16]); the remaining 12 dimensions correspond to the accretion disk radii for each system.

Initialization is accomplished by placing our ensemble of walkers in a tight ball around a best guess that corresponds to the best known estimates of the binary parameters (M_1, q, $P_{\rm orb}$) for each system. If a reliable estimate of M_1 is not known for a system, then the mean of the Ozel mass distribution[52] is used. Similarly, if q is not known for a system, then the median of the uniform distribution between the minimum and maximum of the known values of mass ratio for all dynamically confirmed black holes in the Galaxy[16] is used.

Our hierarchical model samples accretion disk radii from a uniform distribution between the circularization radius ($R_{\rm circ}$) and the radius of the Roche lobe of the compact object (R_1) in the system, both of which depend on only M_1, q and $P_{\rm orb}$. Initial values of $R_{\rm h,disk}$ are set as the median of the uniform distribution between $R_{\rm circ}$ and R_1 for each system, calculated using the best guess for M_1 and q (discussed above), and the known $P_{\rm orb}$.

The prior distributions for each of the 24 parameters are also set using the best-guess orbital parameters for each binary system. If a constrained measurement of the parameter exists (that is, a value with uncertainty), then a Gaussian prior based on this measurement and its uncertainty is used. If only a range is quoted in the literature for a parameter, then a uniform prior is used. The prior distributions for $R_{\rm h,disk}$ are taken as the uniform distribution between $R_{\rm circ}$ and R_1 for each system.

After initialization, we begin running *emcee* on the observed data ($\tau_{\rm e}$) with a 500-step burn-in phase. After this phase, *emcee* is restarted, with the walkers

© 2018 Macmillan Publishers Limited, part of Springer Nature. All rights reserved.

starting at the final position they ended at in the burn-in phase, and run until convergence. Ultimately, *emcee* outputs the converged solution in the form of posterior distributions of α_h for each outburst or system. The converged value and upper and lower limits on this value are taken as the median and 1σ confidence interval of each posterior distribution, respectively; see Extended Data Table 2.

Data availability. The datasets generated during and analysed during this study are available from the corresponding author on reasonable request.

31. Evans, P. A. *et al.* Methods and results of an automatic analysis of a complete sample of Swift-XRT observations of grbs. *Mon. Not. R. Astron. Soc.* **397,** 1177–1201 (2009).
32. Evans, P. A. *et al.* An online repository of Swift/XRT light curves of gamma-ray bursts. *Astron. Astrophys.* **469,** 379–385 (2007).
33. Toor, A. & Seward, F. D. The Crab nebula as a calibration source for x-ray astronomy. *Astron. J.* **79,** 995–999 (1974).
34. Migliari, S. & Fender, R. Jets in neutron star x-ray binaries: a comparison with black holes. *Mon. Not. R. Astron. Soc.* **366,** 79–91 (2006).
35. Foreman-Mackey, D., Hogg, D. W., Lang, D. & Goodman, J. emcee: the MCMC hammer. *Publ. Astron. Soc. Jpn* **125,** 306–312 (2013).
36. Goodman, J. & Weare, J. Ensemble samplers with affine invariance. *Comm. App. Math. Comp. Sci.* **5,** 65–80 (2010).
37. King, A. R. & Ritter, H. The light curves of soft x-ray transients. *Mon. Not. R. Astron. Soc.* **293,** L42–L48 (1998).
38. Menou, K., Hameury, J.-M., Lasota, J.-P. & Narayan, R. Disc instability models for X-ray transients: evidence for evaporation and low a-viscosity? *Mon. Not. R. Astron. Soc.* **314,** 498–510 (2000).
39. Geem, Z., Kim, J. & Loganathan, G. A new heuristic optimization algorithm: harmony search. *Simulation* **76,** 60–68 (2001).
40. Dubus, G., Lasota, J.-P., Hameury, J.-M. & Charles, P. X-ray irradiation in low-mass binary systems. *Mon. Not. R. Astron. Soc.* **303,** 139–147 (1999).
41. Lasota, J.-P. The disc instability model of dwarf novae and low-mass x-ray binary transients. *New Astron. Rev.* **45,** 449–508 (2001).
42. de Jong, J., van Paradijs, J. & Augusteijn, T. Reprocessing of x rays in low-mass x-ray binaries. *Astron. Astrophys.* **314,** 484–490 (1996).
43. Truss, M. R., Wynn, G. A., Murray, J. R. & King, A. R. The origin of the rebrightening in soft x-ray transient outbursts. *Mon. Not. R. Astron. Soc.* **337,** 1329–1339 (2002).
44. Torres, M. A. P. *et al.* Observations of the 599 Hz accreting x-ray pulsar IGR J0029l+5934 during the 2004 outburst and in quiescence. *Astrophys. J.* **672,** 1079–1090 (2008).
45. Šimon, V., Bartolini, C., Piccioni, A. & Guarenieri, A. Interpretation of the 1998 outburst of the unique X-ray transient CI Camelopardalis (XTE j0421+560). *Mon. Not. R. Astron. Soc.* **369,** 355–359 (2006).
46. Campana, S., Coti Zelati, F. & D'Avanzo, P. Mining the AqI X-I long-term X-ray light curve. *Mon. Not. R. Astron. Soc.* **432,** 1695–1700 (2013).
47. Heinke, C. O., Bahramian, A., Degenaar, N. & Wijnands, R. The nature of very faint x-ray binaries: hints from light curves. *Mon. Not. R. Astron. Soc.* **447,** 3034–3043 (2015).
48. Powell, C., Haswell, C. & Falanga, M. Mass transfer during low-mass x-ray transient decays. *Mon. Not. R. Astron. Soc.* **374,** 466–476 (2007).
49. Shahbaz, T., Charles, P. & King, A. Soft x-ray transient light curves as standard candles: exponential versus linear decays. *Mon. Not. R. Astron. Soc.* **301,** 382–388 (1998).
50. Yan, Z. & Yu, W. X-ray outbursts of low-mass x-ray binary transients observed in the RXTE era. *Astrophys. J.* **805,** 87 (2015).
51. Lasota, J.-P., King, A. R. & Dubus, G. X-ray transients: hyper- or hypo-luminous? *Astrophys. J.* **801,** L4 (2015).
52. Özel, F., Psaltis, D., Narayan, R. & McClintock, J. The black hole mass distribution in the galaxy. *Astrophys. J.* **725,** 1918–1927 (2010).

© 2018 Macmillan Publishers Limited, part of Springer Nature. All rights reserved.

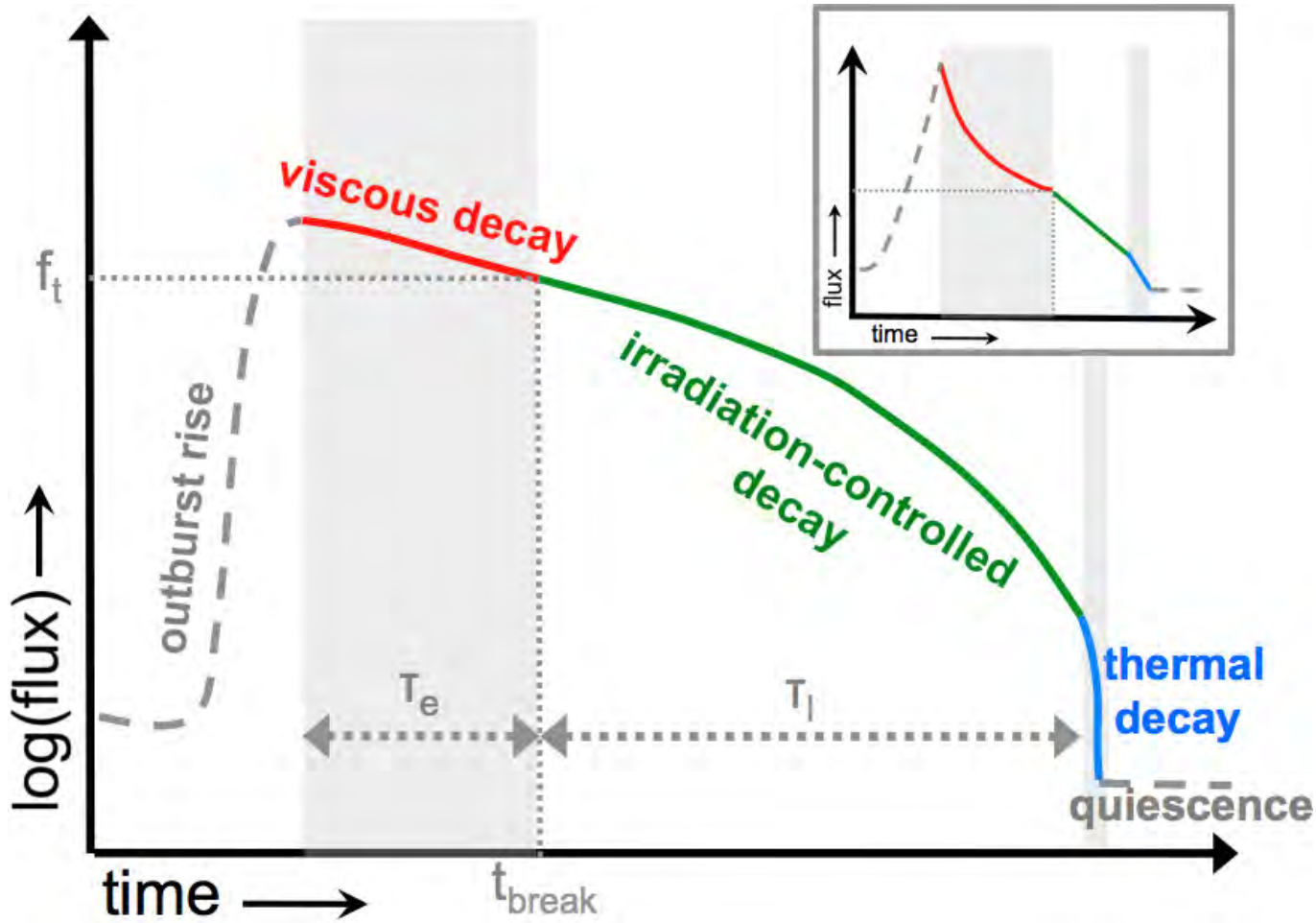

Extended Data Figure 1 | Schematic light curve for an outburst of a low-mass X-ray binary system. The profile shown corresponds to the light curve predicted by the (irradiated) disk-instability model for an outbursting irradiated disk. τ_e and τ_l represent the timescales of the exponential (viscous) and linear (irradiation-controlled) decay stages in the light curve, respectively. The time and flux at which the transition between the viscous and exponential stages of the decay occurs (marking the point at which the temperature in the outer disk drops below the ionization temperature of hydrogen) are represented by t_{break} and f_t, respectively. The inset shows the same light-curve profile on a linear scale.

© 2018 Macmillan Publishers Limited, part of Springer Nature. All rights reserved.

Extended Data Table 1 | Binary orbital parameters for our Galactic black-hole low-mass X-ray binary source sample

Source Name	distance (kpc)	M_1 ($M_\odot$)	q (M_2/M_1)	$P_{\rm orb}$ (hrs)
XTE J1118+480	1.72 ± 0.1	7.2 ± 0.72	0.024 ± 0.009	4.1
MAXI J1305−704	-	-	-	9.74
Swift J1357.2−0933	1.5–6.3	12.4 ± 3.6	-	2.8
GS 1354−64	-	-	0.12±0.04	61.1
4U 1543−475	7.5±0.5	9.4±2.0	0.25–0.31	26.8
XTE J1550−564	4.4±0.5	10.39±2.3	0.031–0.037	37.0
XTE J1650−500	2.6±0.7	4.7±2.2	-	7.7
MAXI J1659−152	1.6–8.0	-	-	2.414
GX 339−4	8.0±2.0	-	-	42.1
Swift J1745−26	-	-	-	≤21
MAXI J1836−194	-	-	-	<4.9
XTE J1859+226	8±3	10.83±4.67	-	6.6

When no acceptable estimates of distance, black-hole mass M_1 or binary mass ratio q are available (indicated by dashes), known Galactic distributions[16,52] are used.

© 2018 Macmillan Publishers Limited, part of Springer Nature. All rights reserved.

Extended Data Table 2 | Quantities derived to describe the mass-transport process in the accretion disks of outbursting low-mass X-ray binaries

Source Name	Outburst ID	τ_e (days)	$R_{\rm disc}$ ($\times 10^{10}$ cm)	α_h	Accretion State(s) Reached	Max Eddington Fraction
4U1543−475	2002	58.94 ± 0.42	$27.91^{+12.2}_{-10.1}$	$0.66^{+0.16}_{-0.14}$	H,I,S	0.16
GS1354−64	2015	$139.69^{+0.63}_{-0.65}$	$52.10^{+18.1}_{-15.3}$	$0.362^{+0.070}_{-0.066}$	H	0.085[a,b]
GX339−4	1996-1999	$167.17^{+2.12}_{-2.31}$	$37.30^{+15.6}_{-14.2}$	$0.250^{+0.059}_{-0.056}$	H,I,S	0.011[a]
	2008	$168.24^{+5.89}_{-5.81}$	$37.24^{+15.5}_{-14.1}$	$0.247^{+0.061}_{-0.056}$	H	0.0059[a]
	2009	$166.88^{+4.96}_{-4.48}$	$37.33^{+15.4}_{-14.1}$	$0.249^{+0.060}_{-0.057}$	H	0.0088[a]
	2013	$172.37^{+3.14}_{-3.51}$	$37.29^{+15.2}_{-14.0}$	$0.242^{+0.058}_{-0.054}$	H	0.014[a]
	2014/2015	$188.90^{+0.25}_{-0.23}$	$37.20^{+15.4}_{-14.0}$	$0.222^{+0.049}_{-0.052}$	H,I,S	0.15[a]
MAXIJ1305−704	2012	$52.90^{+0.11}_{-0.12}$	$12.72^{+5.70}_{-4.65}$	$0.49^{+0.11}_{-0.11}$	H,I,S	0.051[a,b]
MAXIJ1659−152	2010/2011	$60.69^{+1.19}_{-1.23}$	$5.494^{+2.31}_{-2.07}$	$0.265^{+0.059}_{-0.064}$	H,I,S	0.15[a]
MAXIJ1836−194	2011/2012	$93.09^{+1.81}_{-2.00}$	$8.838^{+3.61}_{-3.34}$	$0.220^{+0.049}_{-0.053}$	H	0.11[a,b]
SwiftJ1357.2−0933	2011	$68.31^{+2.16}_{-2.05}$	$6.850^{+3.00}_{-2.46}$	$0.346^{+0.067}_{-0.065}$	H	0.0019
	2017	$64.89^{+3.47}_{-3.68}$	$6.730^{+2.95}_{-2.42}$	$0.366^{+0.066}_{-0.070}$	H	0.00038
SwiftJ174510.8−262411	2012/2013	$81.49^{+1.92}_{-1.86}$	$23.49^{+9.71}_{-8.92}$	$0.410^{+0.097}_{-0.091}$	H	1.2[a,b]
XTEJ1118+480	1999/2000	$85.96^{+0.55}_{-0.56}$	$12.94^{+1.80}_{-2.10}$	$0.279^{+0.017}_{-0.018}$	H	0.0017
	2005	$79.01^{+1.29}_{-1.04}$	$12.95^{+1.78}_{-2.10}$	$0.303^{+0.019}_{-0.021}$	H	0.00047
XTEJ1550−564	2000	$61.78^{+0.38}_{-0.37}$	$55.97^{+10.7}_{-9.53}$	$0.96^{+0.15}_{-0.16}$	H,I,S	0.043
	2001	$61.92^{+5.04}_{-5.79}$	$56.14^{+10.7}_{-9.68}$	$0.962^{+0.101}_{-0.089}$	H,I	0.0068
	2001/2002	$60.38^{+0.64}_{-0.63}$	$56.06^{+10.8}_{-9.60}$	$0.99^{+0.15}_{-0.15}$	H	0.013
	2003	$61.89^{+0.55}_{-0.52}$	$55.99^{+10.7}_{-9.52}$	$0.96^{+0.15}_{-0.14}$	H	0.015
XTEJ1650−500	2001/2002	93.12 ± 1.26	$9.804^{+4.36}_{-3.56}$	$0.185^{+0.034}_{-0.052}$	H,I,S	0.016
XTEJ1859+226	1999/2000	$56.61^{+0.066}_{-0.084}$	$11.62^{+5.23}_{-4.27}$	$0.505^{+0.142}_{-0.093}$	H,I,S	0.18

The efficiency of angular-momentum (and mass) transport α, assuming no mass loss in the hot disk, and related quantities, sampled using our Bayesian hierarchical model, are presented. The accretion state(s) reached in each outburst are indicated as hard (H), intermediate (I) or soft (S).

[a] M_1 is unconstrained, so we assume $M_1 = 10 M_\odot$.

[b] Distance d is unconstrained, so we assume $d = 8$ kpc.

© 2018 Macmillan Publishers Limited, part of Springer Nature. All rights reserved.